1-bit RIS Unit Cell with Mechanical Reconfiguration at 28 GHz

Marcos Baena-Molina, Ángel Palomares-Caballero, Ginés Martinéz-García, Rubén Padial-Allué, Pablo Padilla, Juan F Valenzuela-Valdés

1-bit RIS Unit Cell with Mechanical Reconfiguration at 28 GHz

Marcos Baena-Molina*, Ángel Palomares-Caballero†, Ginés Martinéz-García*, Rubén Padial-Allué‡, Pablo Padilla*, Juan F. Valenzuela-Valdés*

*Department of Signal Theory, Telematics and Communications, Centre for Information and Communication Technologies (CITIC-UGR), University of Granada, 18071 Granada, Spain

†Institut d'Electronique et des Technologies du numéRique (IETR), UMR CNRS 6164, INSA Rennes, France

‡Department of Electronics and Computer Technology, Centre for Information and Communication Technologies (CITIC-UGR), University of Granada, 18071 Granada, Spain

email: marcosb@ugr.es

***Abstract*—In this paper, a mechanically tunable unit cell for reconfigurable intelligent surfaces (RIS) is presented. The RIS unit cell design is based on a metallic cylinder with a metallic cone-shaped element placed at one end. Thanks to the two positions provided by the mechanically reconfigurable cylinder, the cone-shaped element produces a phase shift in reflection of 180º at 28 GHz and therefore, giving the 1-bit reconfiguration. A comparison of the cone-shaped element with other types of geometries such as a cube and a cylinder has been performed. Besides, in view of the unit cell design, a cost-effective fabrication using 3-D printing and spray metallization is considered. A study of dimensional tolerances and conductivity values for the proposed RIS unit cell is done. The simulated results show the robustness of the RIS unit cell for both main dimensions and conductivity values for a frequency range between 25 GHz and 30 GHz.**

***Index Terms*—3-D printing, mechanical reconfiguration, millimeter-wave frequencies, reconfigurable intelligent surface (RIS).**

I. Introduction

Reflectarray (RA) antennas are receiving a lot of attention nowadays thanks to their easy feeding and high directivity, among other advantages they offer. RAs allow either fixed or tunable radiation performance depending on whether the elements that form their structure, called unit cells, have implemented any reconfiguration mechanism. In [1], [2], different reconfiguration elements that modify the reflection phase provided by RA unit cells are described. Some of the reconfigurable elements most commonly used in the RA unit cells are PIN diodes or varactors [3], [4]. Depending on the voltage (in direct current) provided at the terminals of these reconfigurable elements, a variation in the capacitance of their equivalent circuit is produced [4]. In this manner, the electromagnetic (EM) behavior of the RA unit cell changes.

Another of the strategies applied in the design of reconfigurable RAs is the use of mechanically tunable elements [5]. In this case, a mechanical actuator is incorporated in each of the RA unit cells allowing the spatial variation of the unit cell (or any part of it) in such a way that the desired phase shift is achieved. In general, the mechanically reconfigurable elements have longer time responses compared to other alternatives such as diode-based tunable elements. However, mechanically reconfigurable elements have the advantage that the tunable mechanism rarely affect the unit cell behavior due to the positions of the actuators which are, in general, located below the reflecting part. Thanks to this and in contrast to the elements that form the diode-based RAs, the element loss in mechanically reconfigurable RAs is significantly reduced.

There are some mechanically reconfigurable RA designs reported in the literature. A distinction can be made according to the polarization of the incident wave impinging on the RA, whose phase will be locally modified. On the one hand, we have the RA designs that modify the reflected phase of a linearly polarized wave. In [6], [7], the vertical position of a patch antenna with and without slots, respectively, is modified to achieve the full range of phase shift needed for the RA design. Conversely, in the work presented in [8], the minimum phase shift for the RA is achieved through the 90º rotation of the unit cell. In a different way, in [9], four different values of phase shift in the RA unit cell are obtained by moving metal pins under a patch. On the other hand, the following RA designs allow the modification of the reflected phase of an impinging wave with circular polarization. In all of them, a motor located in the unit cell rotates an element to achieve the desired phase shift in the reflected wave. In [10], the rotated element is a patch with the shape of a concentric dual split ring. Differently, in [11], the element, which is rotated to achieve a phase shift range of 360º, is an elliptical inner conductor surrounded by a circular outer conductor. Another example of a mechanically reconfigurable element for RA is presented in [12], which consists of a metallic helix with two branches. In most of the previous works of RAs with mechanical reconfiguration, it can be seen that their operating frequency is below 20 GHz.

Recently, the use of reconfigurable RAs is playing an important role in the conception of the future communication paradigm based on reconfigurable intelligent surfaces (RIS) [13]. In a general way, RIS can be considered as reconfigurable RAs whose excitation is a plane wave and whose unit cells provide discrete phase states. By discretizing the phase shift range to a few values, the complexity and cost of the RIS

decreases in exchange for reducing the directivity provided [14]. In the range near millimeter-wave frequencies, there are some RIS designs [15]–[17]. The unit cells, which constitute the RIS, have an electronic reconfiguration by using PIN diodes. In this paper, a new unit cell design for mechanically RIS is proposed. The proposed RIS unit cell achieves a 180° phase shift at 28 GHz by means of mechanical reconfiguration. Moreover, thanks to its design, its fabrication becomes cost-effective.

II. Mechanically RIS Unit Cells

The proposed RIS unit cell is shown in Figs. 1(a) and 1(b). It consists of a metallic cylinder whose end has a conical shaped element. This metal cylinder is inserted into a cylindrical cavity that allows the movement of the cylinder in the z-direction. The displacement in the z-direction of the cylinder, and also of its cone-shaped end, is represented by the parameter. In Figs. 1(c) and 1(d), two other designs similar to the one described above are displayed but with the difference of the geometry chosen for the element at the end of the cylinder. In Figs. 1(c) and 1(d), the shapes of the elements placed at the end of the cylinder are a cube and cylinder, respectively. It is important to note that the maximum dimensions of these elements, represented by the D parameter, are smaller than the periodicity in both the x- and y- directions defined by the p parameter. This geometrical condition must be fulfilled so that the mechanically reconfigurable element does not encounter any obstacles in its movement due to the neighboring unit cells. All the elements shown in Fig. 1 are made of metal. For the simulation of the described unit cells, the EM software CST Studio Suite is used. The simulation conditions for the unit cells are as follows. *Unit cell* boundary conditions are set in the x- and y- directions, and *open add space* conditions in the z-direction. The solver used for all simulations in this paper is the frequency solver, whose excitation is selected to be a plane wave in $-z$-direction. Since it is a unit cell with RIS application, the results focus on the wave reflected by the unit cell in the $+z$-direction.

Fig. 2 shows a comparison of the EM behavior among the unit cells presented in Fig. 1. Figs. 2(a) and 2(b) illustrate the reflection performance (S_{11}) in magnitude and phase, respectively. More specifically, Fig. 2(b) shows the phase shift produced by the RIS unit cell between its two possible states, i.e. $m = 3$ mm (state "0") and $m = 0$ mm (state "1"). It can be seen that there are differences in behavior between unit cells depending on the geometry of the element located at the end of the cylinder. The biggest differences are found for the state "0" since, depending on the geometry used, a resonance appears earlier or later in frequency. This resonance is important since it marks a change in the trend of the phase response in frequency and consequently, of the phase stability along the frequency as can be seen in Fig. 2(b). The cone-shaped geometry is the one that pushes further the frequency resonance, approximately up to 31 GHz. This allows a phase shift of 180°$\pm$ 20° to be achieved from about 25 GHz to 31 GHz as can be seen in Fig. 2(b) for the unit cell with

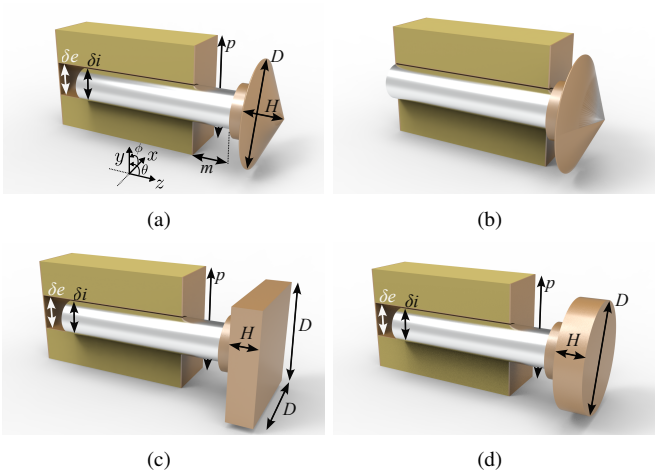

Fig. 1. 3-D views of mechanically RIS unit cells. (a) Proposed unit cell with cone-shaped end in state "0", (b) unit cell with cone-shaped end and in state "1", (c) unit cell with cube-shaped end and, (d) unit cell with cylinder-shaped end. The dimensions (in mm) are: $D = 8.04$ mm, $H = 1.95$ mm, $p = 9$ mm, $\delta_e = 3$ mm and $\delta_i = 2.9$ mm.

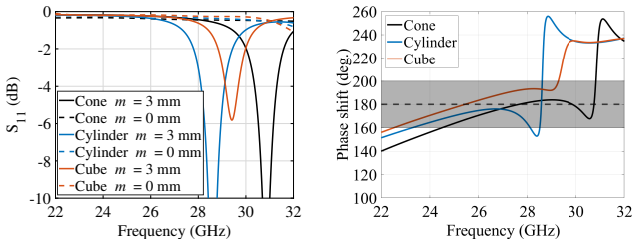

Fig. 2. Simulated reflection performance of the mechanically RIS unit cells. (a) In magnitude and, (b) phase shift between the two states of the unit cells.

cone-shaped end. The unwanted resonance, which appears for the state "0" of all unit cells, is formed between the end of the cavity supporting the cylinder and the back of the element located at the end of the cylinder. In this region of space, the electric field is confined at the resonant frequency. The boundary conditions that allow this resonance to exist depend on both the parameter m and the profile of the element at the end of the cylinder.

III. RIS Unit Cell with Cone-Shaped End

As discussed in the previous section, the element chosen to be placed at the end of the cylinder is the cone. Due to its geometry, this element can be manufactured in a simple, repetitive and adaptable way by 3-D printing in plastic and then, a metal coating. The cylinder that moves this element will be implemented by a commercial electromagnet, which depending on its power bias will move the element to the "0" or "1" state. In this section, an analysis is carried out on how the EM performance (discussed in the previous section) is affected by the possible tolerances of the selected fabrication process.

A. Tolerance analysis

For the 3-D fabrication of the cone-shaped element, 3-D printing based on stereolithography (SLA) has been chosen. More specifically, the printer to be used is the Form 3 from Formlabs. This printer has a resolution in the XY plane of 25 μm, a laser spot of 85 μm and an adjustable layer thickness of at least 25 μm. The material to be used in the printing process is the grey V4 resin. According to the dimensional accuracy report made by Formlabs on this printer [18], for geometries up to 9 mm, the standard deviation is up to 0.03 mm. With this information, a tolerance study is performed on the geometry of the cone-shaped element. Fig. 3 shows the performance in magnitude and phase shift provided by the two states of the unit cell when varying 0.5 mm the main dimensions of the element, these are D and H [see Fig. 1(a)]. The dimensional variation chosen to make the analysis is much larger than the standard deviation of the 3-D printer but in this way, the robustness of the printed element will be assessed in extreme cases. According to the simulated results in Fig. 3, they show a slight variation in the position of the resonance and thus, in the phase shift provided between unit cell states. To facilitate the visual comparison of this variation, the black curves represent the performance of the unit cell in the reference case, i.e. the one presented in Fig. 2. In all the cases presented in Fig. 3, as the diameter D of the cone-shaped element decreases, the phase shift value is reduced. This is because the surface area to reflect the incident wave is reduced and thus, the proportion of the reflected power that is affected by the reconfigurable element also decreases. It can be concluded that the tolerance study indicates that even with large deviations in the main dimensions of the cone-shaped element, it preserves the expected EM performance from 26 GHz to 30 GHz, approximately.

Concerning the behavior of the RIS element with the angle of incidence, since the distance between elements is relatively large ($0.84\lambda_o$ at 28 GHz), the maximum scan angle free from grating lobes is approximately 10°. This angular value can be increased if a smaller distance between RIS elements is achieved. This fact is closely related to the miniaturization of the mechanical actuator, which is the one that establishes the minimum possible period in the RIS.

After analyzing the modifications in the reflection performance when varying the dimensions of the printed element, we will study the effects of applying a metal coating with different conductivity values σ. It is important to note that the above results discussed in Figs. 2, 3 and 4 correspond to a $\sigma = 10^4$ S/m. To perform a cost-effective metallization, we are going to use the following metallizing spray [19], which is silver plated copper compound. According to its datasheet, this spray can provide a conductivity from $7{\cdot}10^4$ S/m to $2{\cdot}10^4$ S/m for a metallization thickness of 50 μm. As we did in the tolerance study in Fig. 3, Fig. 4 presents the performance in magnitude and phase when the conductivity varies beyond this range of conductivity provided by the datasheet of the spray. In this way, we see how robust the proposed RIS unit

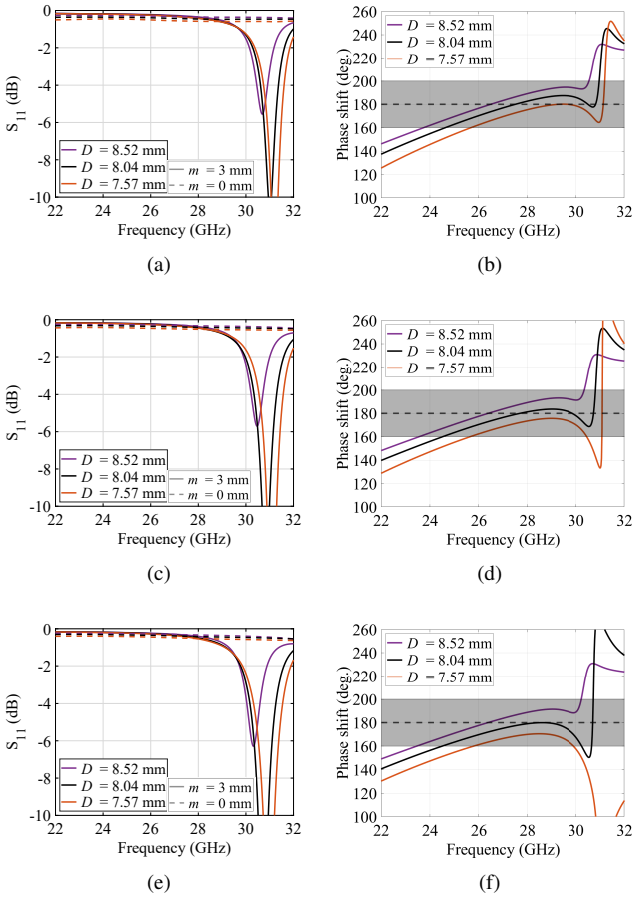

Fig. 3. Reflection performance of the RIS unit cell with cone-shaped end when parameters D and H are modified. Reflection performance in magnitude when D varies and (a) H =1.45 mm, (c) H =1.95 mm and, (e) H = 2.45 mm. Reflection phase shift when D varies and (b) H =1.45 mm, (d) H =1.95 mm and, (f) H = 2.45 mm.

cell is to changes in the conductivity value of the applied coating. From Fig. 4, it can be noted that even with very low conductivity values, as in the cases of $\sigma = 10^3$ S/m and $\sigma = 10^2$ S/m, the expected behavior in magnitude and phase is maintained from about 25 GHz to 29 GHz, approximately. It should be pointed that for the lowest conductivity value and at the highest frequency (29 GHz), i.e., the worst case, the reflection losses are approximately -4 dB. Nonetheless, once the element is fabricated and metallized, as a worst case, we expect to obtain a conductivity similar to the orange curve in Fig. 4.

The robustness in the EM response of the proposed RIS unit cell over a wide range of conductivity values is mainly due to the mechanism that provides the reflection. For our RIS unit cell, this mechanism is a mismatching between the free space and the conductive surface of the cone-shaped element. An analysis of reflection level with respect to the thickness of a metal with certain conductivity can be found in [20].

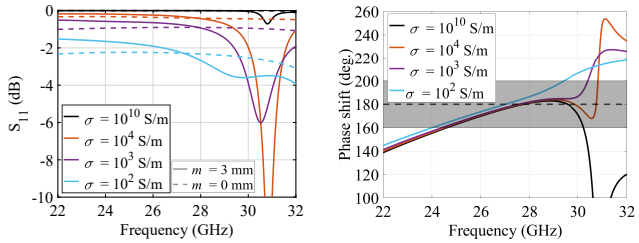

(a) (b)

Fig. 4. Reflection performance of the RIS unit cell with cone-shaped end when the conductivity value of the cone varies. (a) In magnitude and, (b) phase shift between the two states of the unit cells. The dimensions of the RIS unit cell are the ones indicated in Fig. 1. The considered metallization thickness is 50 μm.

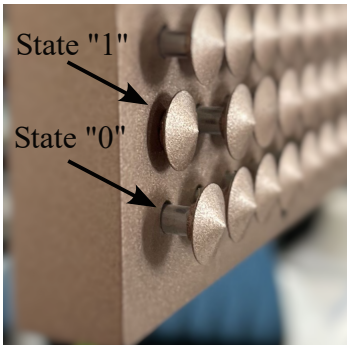

Fig. 5. Photo of the manufactured RIS unit cells with cone-shaped end. The two possible states of the proposed RIS unit cell have been indicated as state "0" and state "1".

B. Manufacturing

As discussed above, a fabrication process based on 3-D printing plus a subsequent metal coating was used to manufacture the RIS unit cell in Fig. 1(a). The result can be seen in Fig. 5, where an array of RIS unit cells with cone-shaped end is illustrated. Specifically, the SLA-based 3-D printer has been used for the realization of the cone-shaped element and for the support surrounding the metal cylinder, which applies the movement to the cone-shaped element. A thin layer of metallization has been applied to these two pieces of the RIS unit cell using the metallic spray discussed in the previous section. The application of the spray is of short duration of time in order to obtain a thickness for the metallization of several tens of microns. This value is not controlled but, since the spray is conductive (in the order of 10^4 S/m), it is sufficient to have a few microns of thickness to have a proper reflection [20]. For the implementation of the cylinder that produces the two states, an electromagnet has been used which can move freely inside the 3-D printed holder. Fig. 5 also illustrates the two possible states that can be produced with the proposed mechanically RIS unit cell design.

IV. Conclusion

This paper has presented a mechanically tunable unit cell for reconfigurable intelligent surfaces (RIS). The proposed RIS unit cell, which is mainly composed of a metallic cylinder with a cone-shaped element at one of its ends, offers two mechanically reconfigurable positions. The difference in reflection phase response of the two possible positions results in a 180º phase shift, i.e., 1-bit reconfiguration capability. Through a comparison with alternative geometric shapes like cubes and cylinders, we have demonstrated the superiority of our cone-shaped element design for the reflection performance over the frequency. Moreover, we have explored a cost-effective fabrication approach employing 3-D printing based on SLA and spray metallization with moderate conductivity value. To verify that this type of fabrication is valid for the proposed RIS unit cell, a study of dimensional tolerances and conductivities has been performed. It has been observed from the simulated results that the desired reflection level in magnitude and the phase shift is preserved from 25 GHz to 30 GHz. Finally, a first successful fabrication of an array of RIS unit cell with cone-shaped end has been achieved through the described fabrication techniques.

Acknowledgment

This work has been supported by grant PID2020-112545RB-C54 funded by MCIN/AEI/10.13039/501100011033. It has also been supported by the Brittany Region under Contract SAD 22006912 (SuMeRIO), grants PDC2022-133900-I00, TED2021-129938B-I00 and TED2021-131699B-I00 funded by MCIN/AEI/10.13039/501100011033 and by the European Union NextGenerationEU/PRTR.

References

[1] S. V. Hum and J. Perruisseau-Carrier, "Reconfigurable reflectarrays and array lenses for dynamic antenna beam control: a review," *IEEE Trans. Antennas Propag.*, vol. 62, no. 1, pp. 183-198, Jan. 2014.

[2] W. Disharoon, S. Y. Lee, J. Ramsey and N. Ghalichechian, "Overview of reconfiguration technologies for reflectarrays and trasmitarrays," in *2023 17th European Conference on Antennas and Propagation (EuCAP)*, Florence, Italy, 2023.

[3] J. Han, L. Li, G. Liu, Z. Wu and Y. Shi, "A wideband 1 bit 12 × 12 reconfigurable beam-scanning reflectarray: design, fabrication, and measurement," *IEEE Antennas Wirel. Propag. Lett.*, vol. 18, no. 6, pp. 1268-1272, June 2019.

[4] F. Venneri, S. Costanzo and G. Di Massa, "Design and validation of a reconfigurable single varactor-tuned reflectarray," *IEEE Trans. Antennas Propag.*, vol. 61, no. 2, pp. 635-645, Feb. 2013.

[5] M. Mirmozafari *et al.*, "Mechanically reconfigurable, beam-scanning reflectarray and transmitarray antennas: A review," *Appl. Sci.*, vol. 11, no. 15, p. 6890, Jul. 2021.

[6] X. Yang *et al.*, "A Mechanically reconfigurable reflectarray with slotted patches of tunable height," *IEEE Antennas Wirel. Propag. Lett.*, vol. 17, no. 4, pp. 555-558, April 2018.

[7] Weixiong Luo, Shixing Yu, Na Kou, Zhao Ding, and Zhengping Zhang, "Design of height-adjustable mechanically reconfigurable reflectarray," *Prog. Electromagn. Res. Lett.*, Vol. 104, 1-6, 2022.

[8] P. Mei, S. Zhang and G. F. Pedersen, "A low-cost, high-efficiency and full-metal reflectarray antenna with mechanically 2-D beam-steerable capabilities for 5G applications," *IEEE Trans. Antennas Propag.*, vol. 68, no. 10, pp. 6997-7006, Oct. 2020.

[9] D. E. Serup, G. F. Pedersen and S. Zhang, "Electromagnetically controlled beam-steerable reflectarray antenna," *IEEE Trans. Antennas Propag.*, vol. 71, no. 5, pp. 4570-4575, May 2023.

[10] X. Yang *et al.*, "A broadband high-efficiency reconfigurable reflectarray antenna using mechanically rotational elements," *IEEE Trans. Antennas Propag.*, vol. 65, no. 8, pp. 3959-3966, Aug. 2017.

[11] S. Bi, L. Xu, X. Cheng, Y. Sun, Q. Zhang and C. Yuan, "An all-metal, simple-structured reflectarray antenna with 2-D beam-steerable capability," *IEEE Antennas Wirel. Propag. Lett.*, vol. 22, no. 1, pp. 129-133, Jan. 2023.

[12] G. Kong, X. Li, Q. Wang and J. Zhang, "A wideband reconfigurable dual-branch helical reflectarray antenna for high-power microwave applications," *IEEE Trans. Antennas Propag.*, vol. 69, no. 2, pp. 825-833, Feb. 2021.

[13] Y. Liu *et al.*, "Reconfigurable intelligent surfaces: principles and opportunities," *IEEE Commun. Surv. Tutor.*, vol. 23, no. 3, pp. 1546-1577, thirdquarter 2021.

[14] H. Yang *et al.*, "A study of phase quantization effects for reconfigurable reflectarray antennas," *IEEE Antennas Wirel. Propag. Lett.*, vol. 16, pp. 302-305, 2017.

[15] V. Popov *et al.* "Experimental demonstration of a mmWave passive access point extender based on a binary reconfigurable intelligent surface," *Frontiers in Communications and Networks*, vol.2, 733891, 2021.

[16] J. H. Oh, J. Jeong, Y. Park and S. -H. Wi, "A 29 GHz dual-polarized reconfigurable intelligent surface with 2-dimensional wide scanning range," in *2023 17th European Conference on Antennas and Propagation (EuCAP)*, Florence, Italy, 2023.

[17] R. Wang, Y. Yang, B. Makki and A. Shamim, "A Wideband reconfigurable intelligent surface for 5G millimeter-wave applications," *arXiv preprint*, arXiv:2304.11572 (2023).

[18] *Form 3 Dimensional Accuracy Report*, Formlabs. [Online]. Available: https://3d.formlabs.com/form-3-dimensional-accuracy-report/

[19] *RS 247-4251 Aerosol DataSheet. Silver Coated Copper Screening Compound*. Accessed: Oct., 2023. [Online]. Available: https://docs.rs-online.com/16c4/0900766b8158361e.pdf

[20] A. Roehrner, G. Strauss and T. Eibert, "A broadband inhomogeneous frequency selective surface on quartz glass substrate," in *2022 16th European Conference on Antennas and Propagation (EuCAP)*, Madrid, Spain, 2022.